Journal of Engineering Science and Technology
Vol. 6, No. 4 (2011) 429 - 444

STUDY OF HEAT AND MOISTURE DIFFUSION THROUGH A WALL EXPOSED TO SOLAR HEAT FLUX

Y. TAMENE[1,2,*], S. ABBOUDI[2], C. BOUGRIOU[1]

[1]Laboratoire d'Etude des Systèmes Energétiques Industriels, Département de Mécanique
Université Hadj Lakhdar, Rue Chahid M. El. Hadi Boukhlouf, 05000 Batna, Algérie
[2]Laboratoire Systèmes et Transports (SET), Département Génie Mécanique et Conception,
Université de Technologie Belfort Montbéliard, site de Sévenans, 90010 Belfort Cedex, France
*Corresponding Author: tamene_y@yahoo.fr

Abstract

A numerical study of the heat and mass transfer through a wall is proposed in this work. The studied wall is submitted to mass and heat convective exchange with the ambient. One of its sides is submitted to a variable solar heat flux. The computer program is used to compare the cases of coupling and no coupling heat and mass transfer through the wall under variable heat flux and ambient temperature. The temperature effect on the moisture diffusion and vice versa is presented for two usual materials. An optimal proposal can be clear from this study based on objectives which are mainly the reductions of energy consumption as it is for winter heating or summer cooling.

Keywords: Coupling, Diffusion, Heat, Humidity, Solar flux, Unsteady, Wall.

1. Introduction

The heat and mass transfer in building is very important because it has a big impact on energy economy, occupant's health and building materials damage. It appears also in other fields such as engineering, energy systems including heat exchangers, aerospace, electronics and other thermal devices. The area of building has been the subject of interest for many researchers. Mendes et al. [1] have shown the effects of moisture on sensible and latent conduction loads by using a simple heat and mass transfer model with variable material properties, under varying boundary conditions. He also presents a new mathematical method for this kind of problem, with an unconditionally stable numerical method [2]. Sami et al. [3] approached the problem of power consumption side in the hot zone for cooling the building where it took as a model Riyadh town

Nomenclatures

C_p	Specific heat, J/kg K
D_T	Mass transport coefficient associated to a temperature gradient, m²/s K
D_{TV}	Vapor phase transport coefficient associated to a temperature gradient, m²/s K
D_θ	Mass transport coefficient associated to a moisture content gradient, m²/s
$D_{\theta V}$	Vapor phase transport coefficient associated to a moisture content gradient, m²/s
h	Heat convection transfer coefficient, W/m^{2}K
h_m	Mass convection transfer coefficient, m/s
L	Wall thickness, m
L_v	Heat of vaporisation, J/kg
N	Node number
P	Pressure, Pa
T	Temperature, °C
T_f	Air temperature, °C
t	Time, s

Greek Symbols

Φ	Absorbed solar flux, W/m^2
λ	Thermal conductivity, W/m K
ρ	Mass density, kg/m^3
θ	Total moisture volumetric content, m^3 of water/m^3 of porous material

Subscripts

L	Liquid
V	Vapour
0	Initial
1	Internal side
2	External side
∞	Far wall

(Saudi Arabia) to optimize the thickness of the insulation using a finite volume computer code.

Experimentally Simonson et al. [4] conducted a comparison between a numerical code and a simplified method for the experimental study of mass and heat transfer for two types of insulation (cellulose, plywood) used in buildings.

Research also affects other areas that involve the mass and heat transfer. Hussain et al. [5] presented an experimental study of tubular ceramic membranes used in the reactor coolant where the thermal influence on mass transfer was discussed. On the other hand, Askri et al. [6] conducted a study on heat and mass transfer in a metal-hydrogen reactor. They used a numerical simulation to present the time–space evolutions of the temperature and the hydride density in the reactor and to determinate the sensitivity to some parameters (absorption coefficient, scattering coefficient, reactor wall emissivity).Where it has shown sensitivity to certain parameters such as absorption coefficient and diffusivity of the reactor wall. Various parameters such as latent heat diffusion and convection coefficients are the few parameters that can influence the distribution of heat and

diffusion of particles as it is moisture or other. The study proposed by Oxarongot [7] has been applied to diesel particulate filters. For the particle diffusion, Fick's law has been used in combination with the heat equation for the specific geometry of the filter. Other studies have been conducted in the field of food; Hamdan et al. [8] developed a numerical simulation to determine the moisture, the temperature and the mass loss during the chilling process. But the habitat is an area where the mass and heat transfer and their coupling is the most studied. A dynamic model for evaluating the transient thermal and moisture transfer behaviour in porous building materials was presented by Qin et al. [9], where heat and moisture transfer are simultaneously considered and their interactions are modelled. An analytical method has been proposed to calculate the coupled heat and moisture transfer process in building materials. Nguyen et al. [10] developed a physically based model describing the coupled ion and moisture transport by combining theories of liquid water and water vapour transport with aqueous electrolyte theory. They derive the set of governing differential equations describing simultaneous movement of water in the vapour and liquid phases and consequent transport of ions in unsaturated porous media. The equations are developed in one-dimension, assuming isothermal conditions. A computer program has been developed to solve this problem.

Dos Santos et al. [11] proposes a two-dimensional mathematical model considering the coupled heat, air and moisture transport through unsaturated building hollow bricks. Simulations for evaluating hydrothermal performance were performed for massive, hollow and insulating bricks. External boundary conditions of temperature and vapour pressure have been taken as sinusoidal functions, while the internal ones have been kept constant. Comparisons in terms of heat and vapour fluxes at the internal boundary have been presented, showing the brick thermal capacity, mass transport and two-dimensionality aspect effects on the sensible latent and total heat transfer through the brick. Zhang et al. [12] studies the thermal performance of the phase change material (PCM) wallboard by theoretical analysis and numerical simulation, where the inner surface heat flux is used to evaluate the thermal performance of the PCM wallboard and other building envelope components.

Ordenes et al. [13] presents a method to estimate the thermal conductivity and volumetric heat capacity of a homogeneous element using a non-destructive test considering natural oscillations. Surface temperature and heat flux are measured in a concrete sample (with known thermal properties) and the data is treated with a signal processing technique. Estimation is carried out with a heat and moisture transfer model.

We have study the heat transfer in multilayered wall exposed to variable solar flux [14], and in this present work, we resolved a coupled heat and mass equations with real boundary conditions (variable solar flux and ambient) and realised a code to study the diffusion of heat and moisture through the wall subject to the real climatic conditions, it was compared and agreed with experimental results obtained in reference [15]. This computer program permitted us to study and see the influence of the coupling between heat and mass transfer on the evolution of the temperature and moisture in presence of variable solar flux and external temperature, because it is faster it can used to see the influence of different parameters on heat and mass evolution through a wall and see the best configuration to optimised the system with the wanted objective.

2. Formulation of the Problem

The model of heat and mass transfer in unsaturated porous media through classical mechanism of vapour diffusion and liquid movement by capillarity is described by Philip and De Vries model [16]:

$$\rho.C_P \frac{\partial T}{\partial t} = \frac{\partial}{\partial x}\left(\lambda \frac{\partial T}{\partial x}\right) + \rho_L L_V \frac{\partial}{\partial x}\left(D_{T_V} \frac{\partial T}{\partial x}\right) + \rho_L L_V \frac{\partial}{\partial x}\left(D_{\theta_V} \frac{\partial \theta}{\partial x}\right) \quad (1)$$

$$\frac{\partial \theta}{\partial t} = \frac{\partial}{\partial x}\left(D_T \frac{\partial T}{\partial x}\right) + \frac{\partial}{\partial x}\left(D_\theta \frac{\partial \theta}{\partial x}\right) \quad (2)$$

where $D_T = D_{T_L} + D_{T_V}$ and $D_\theta = D_{\theta_L} + D_{\theta_V}$

By supposing that thermal conductivity, diffusivity, and mass transport coefficient associated with moisture content gradient are constant, we obtained the following form of Eqs. (1) and (2):

$$\frac{\partial T}{\partial t} = D' \frac{\partial^2 T}{\partial x^2} + S_\theta \quad (3)$$

$$\frac{\partial \theta}{\partial t} = D_\theta \frac{\partial^2 \theta}{\partial x^2} + S_T \quad (4)$$

where:

$$D' = \left(\frac{\lambda + \rho_L L_V D_{T_V}}{\rho.C_P}\right),\ D'_{\theta_V} = \frac{\rho_L L_V D_{\theta_V}}{\rho.C_P},\ S_\theta = D'_{\theta_V} \frac{\partial^2 \theta}{\partial x^2},\ \text{and}\ S_T = D_T \frac{\partial^2 T}{\partial x^2}$$

The associated boundary conditions are illustrated on Fig. 1**.**

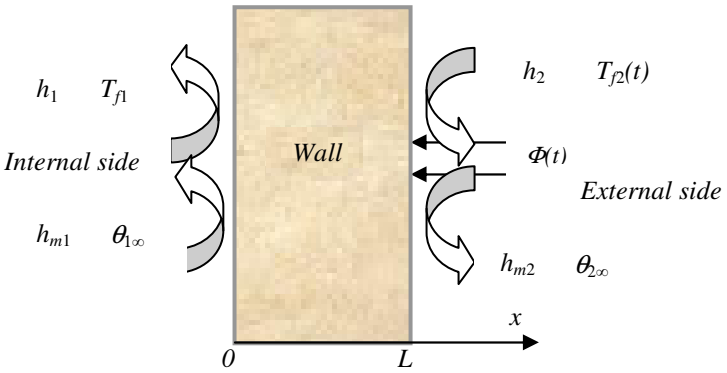

Fig. 1. Presentation of the System.

For mass transfer:

$$-\rho_L D_T \frac{\partial T}{\partial x} - \rho_L D_\theta \frac{\partial \theta}{\partial x} = h_{m_1}(\rho_1 - \rho_{1\infty}) \qquad x = 0 \quad (5)$$

$$-\rho_L D_T \frac{\partial T}{\partial x} - \rho_L D_\theta \frac{\partial \theta}{\partial x} = h_{m_2}\left(\rho_{N\infty} - \rho_2\right) \qquad x = L \qquad (6)$$

For heat transfer:

$$-\lambda \frac{\partial T}{\partial x} - \rho_L L_V D_{T_V} \frac{\partial T}{\partial x} - \rho_L L_V D_{\theta_V} \frac{\partial \theta}{\partial x} = h_1\left(T_{f_1} - T(0)\right) \qquad x = 0 \qquad (7)$$

$$-\lambda \frac{\partial T}{\partial x} - \rho_L L_V D_{TV} \frac{\partial T}{\partial x} - \rho_L L_V D_{\theta_V} \frac{\partial \theta}{\partial x} = h_2\left(T(L) - T_{f\,2}\right) - \Phi(t) \qquad x = L \qquad (8)$$

where the mass convection coefficients h_{m_1} and h_{m_2} are related respectively to the heat transfer coefficients h_1 and h_2 by the Lewis relation. The initial conditions are:

$T_i = T_o$, $\theta = \theta_o$ at $t = 0$, and $0 \le x \le L$ (9)

The mass densities ρ_1, $\rho_{1\infty}$, ρ_2, and $\rho_{2\infty}$ are computed by the following equation:

$$\rho = \frac{p}{R_h T}, \text{ with } R_h = \frac{R_S}{1 - \left(\theta \frac{p_{sat}}{p}\right)\left(1 - \frac{R_S}{R_v}\right)} \qquad (10)$$

R_s = 287.06 J/kg K is the universal gas constant of dry air and

R_v = 461 J/kg K is the universal gas constant of water vapour.

And the saturation vapour pressure p_{sat} is determined by Magnus formula [17]:

$$p_{sat} = 611.213 \exp\left(\frac{17.5043 T}{241.2 + T}\right) \qquad (11)$$

Finally we obtained:

$$\rho(\theta, T, P) = \frac{1}{A}\left[P - B\,\theta \exp\left(\frac{CT}{D + T}\right)\right] \qquad (12)$$

where A =287.06 (T+273.15), B = 230.617, C = 17.5043, and D = 241.2.

3. Numerical resolution

The resolution of the coupled system of Eqs. (1) and (2) with boundary conditions (4), (5), (6) and (7) and initial conditions (8) is performed by finite differences method according to the Cranck-Nicolson scheme [18]. At each time, the Tri Diagonal Matrix Algorithm of Thomas (TDMA) is used to solve the obtained algebraic systems of temperature and humidity following the Flow chart shown in Fig. 2.

The simulated results are obtained for two commonly materials; brick and plywood) used in building construction as shown in Table 1.

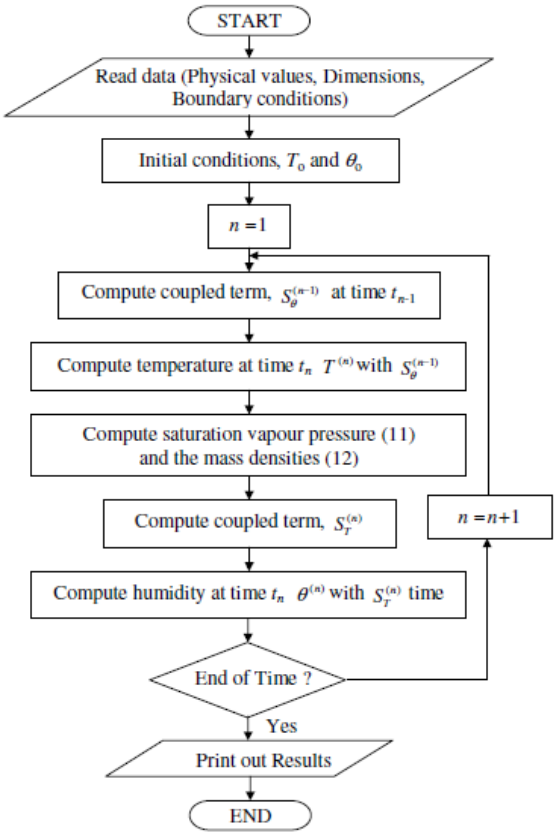

Fig. 2. Flow Chart of the Computer Program.

Table 1. Physical Properties of the chosen Materials.

	Brick [1]	Plywood [4]
ρ, kg/m^3	1900	445
C_p, J/kg K	920	1880
λ, W/m K	1.11	0.091
L, m	0.1	0.02
L_v, J/kg	2.5×10^6	2.5×10^6
D_T, m²/s K	5×10^{-11}	10^{-11}
D_{Tv}, m²/s K	5×10^{-11}	5×10^{-11}
D_θ, m²/s	10^{-7}	4.5×10^{-7}
$D_{\theta v}$, m²/s	10^{-12}	10^{-12}

The values of the boundary conditions used are:

h_1=50 W/m^2 K, h_2=100 W/m^2 K, T_{fl}=15°C, $\theta_{1\infty}$=0.5, and $\theta_{2\infty}$=0.75.

In this work, we consider a periodic variation of the solar heat flux and of the ambient (or air) temperature, Figs. 3 and 4. The solar heat flux is taken zero at night and increases gradually during a journey.

$$\phi(t)=\begin{cases}\Phi_0 \sin(\omega t) & \text{if} \quad 0 \le t \le \tau/2 \\ 0 & \text{if} \quad \tau/2 \le t \le \tau\end{cases} \tag{13}$$

and

$$T_{f_2}(t) = T_{f\,0} + \Delta T \sin(\omega t) \tag{14}$$

where $\omega = 2\pi/\tau$, $\Phi_0 = 500$ W/m², $\tau = 24\,h$, T_{f0}=15°C, and $\Delta T = 10\,°\text{C}$.

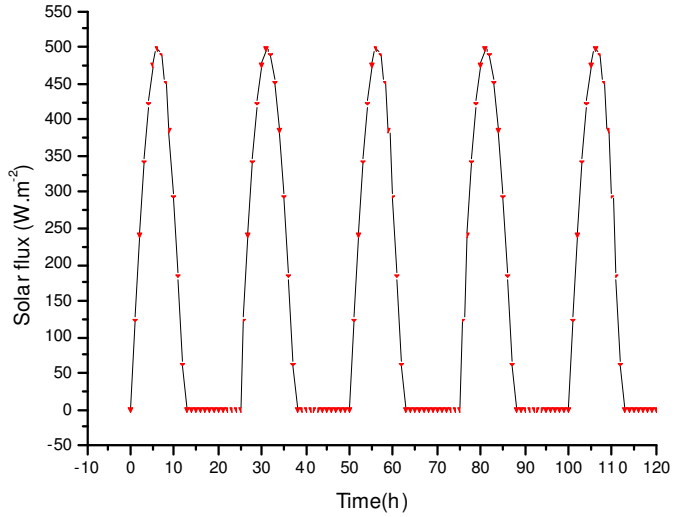

Fig. 3. Solar Heat Flux.

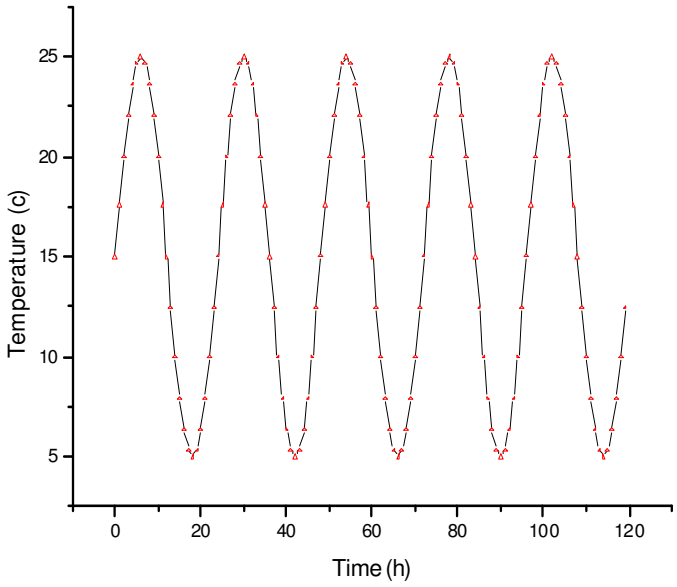

Fig. 4. External Fluid Temperature.

Before exploiting our developed code, we analysed the grid independency of the obtained results. Four test cases are realized with grid numbers N=30, 50, 70 and 100 and time step equal to 36 s. The results are summarized in Table 2 and show that the maximum errors of temperature and humidity are respectively of the order 10^{-4} and 10^{-3} between cases N=50 and N=70. Afterwards, we kept the value N=50.

Table 2. Grid Independency Analysis.

N	30	50	70	100
T_2 °C	15.6821	15.6819	15.6819	15.6819
T_1 °C	15.7498	15.7501	15.7502	15.7504
θ_2	0.72622	0.73601	0.74009	0.74311
θ_1	0.5	0.50001	0.50002	0.50004

4. Results and Discussion

Firstly we present respectively in Figs. 5(a) and 5(b) the temperature evolution for different Reynolds numbers obtained experimentally by Prabal et al. [4] and our code at the same conditions. The initial and outdoor values of moisture and temperature are given in Table 5.2 of [15]. The comparison between the two figures shows a good agreement between the two approaches.

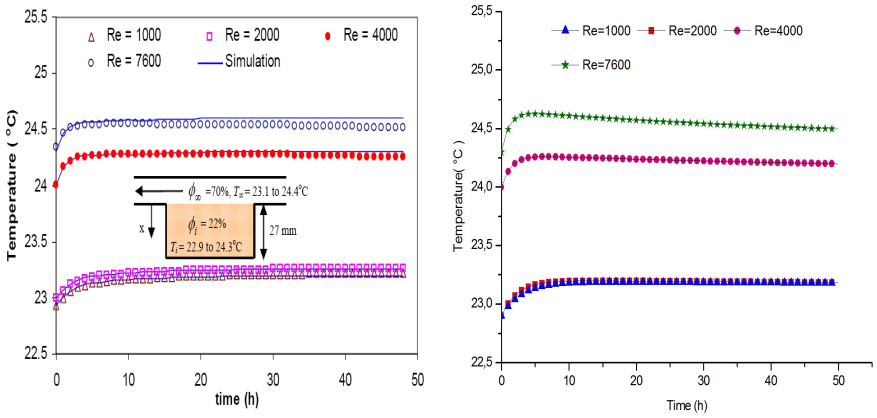

(a) (b)

Fig. 5. Temperature Evolution for Different Reynolds Numbers.

Figures 6 and 7 show that the external and internal temperatures are reduced by the presence of moisture. This reduction is far more at the inside than the outside wall. This result can be explained by the fact that the external temperature is relatively greater than the internal, thus reduces more the effect of moisture.

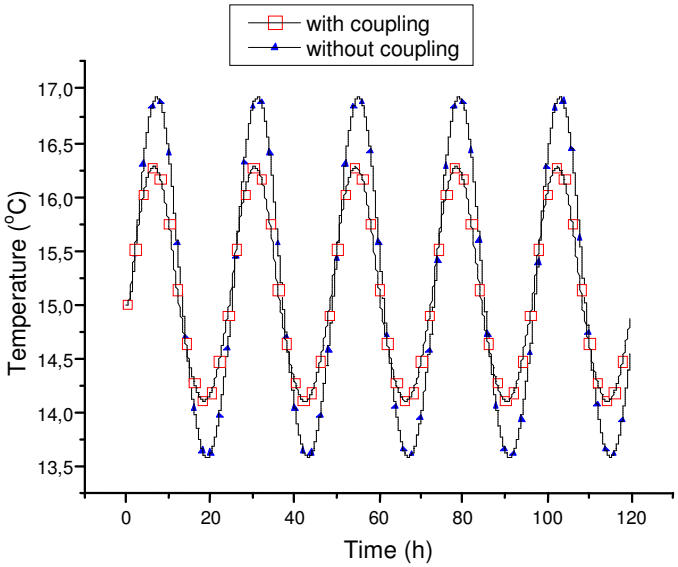

Fig. 6. Internal Temperature (Brick).

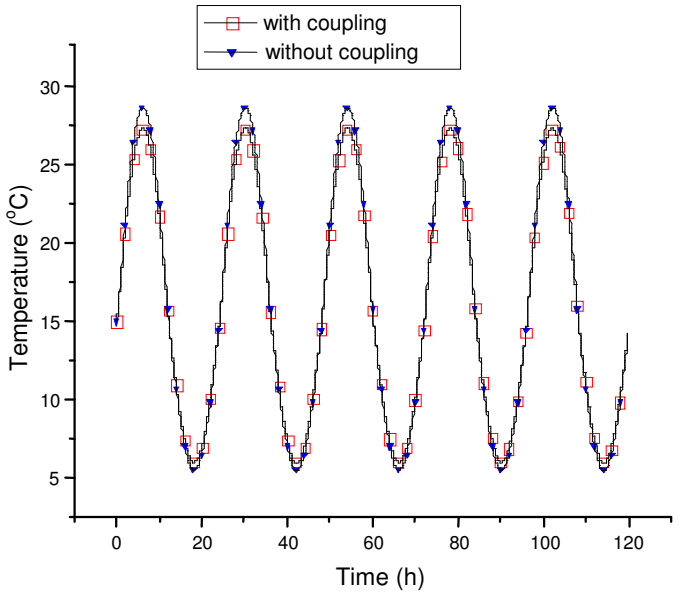

Fig. 7. External Temperature (Brick).

Figures 8 and 9 show clearly that the temperature decreases the diffusion of moisture that is on the internal face or the external face. We note that the moisture changes at the external side faster than at the internal side. This result can be explained by the fact that the wall thickness decreases the moisture transfer and thus, it takes more time to attain the internal side.

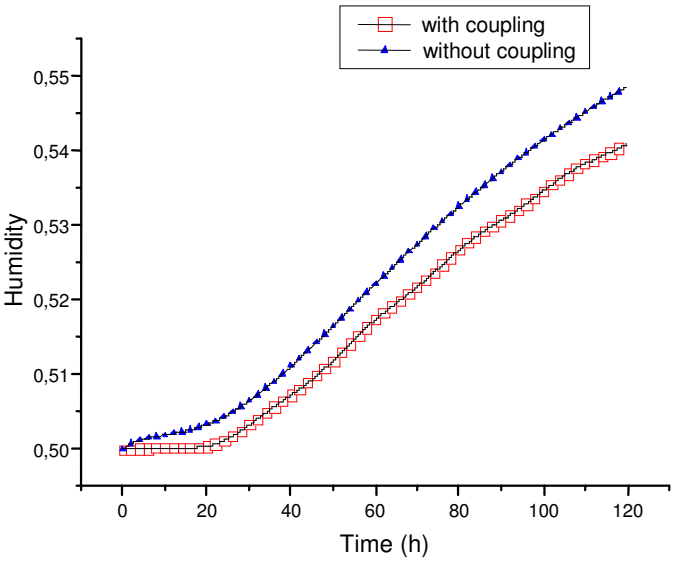

Fig. 8. Internal Humidity (Brick).

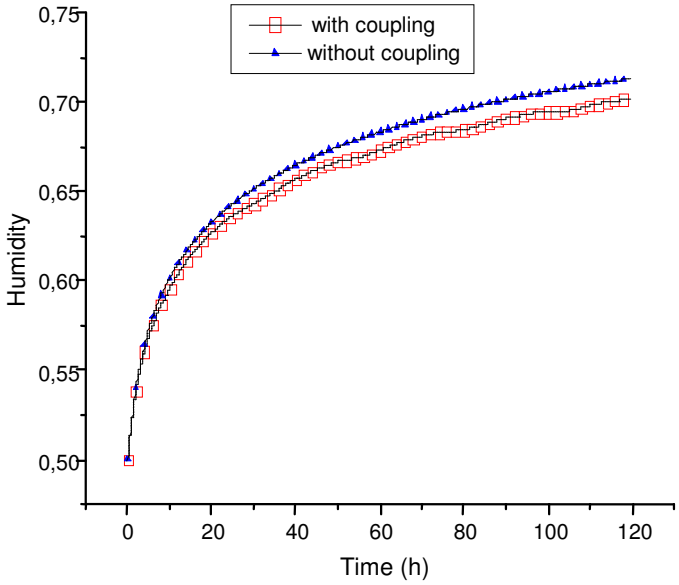

Fig. 9. External Humidity (Brick).

On the other hand, for the adiabatic wall, Fig. 10 allowed us to see that the temperature of the inside face is less influenced by the moisture compared to the outer face, Fig. 11. We note also, that the internal temperature of the adiabatic wall (plywood) is less than that of brick despite the great difference in their thicknesses, 2 cm and 10 cm respectively. So, there's a noticeable influence of the temperature on the moisture migration that is decreased in an apparent manner at the outside face, Fig. 12 and the inside face of the wall, Fig. 13. Also, we clearly

observe the effect of the sinusoidal variations of the ambient temperature and heat flux on the moisture.

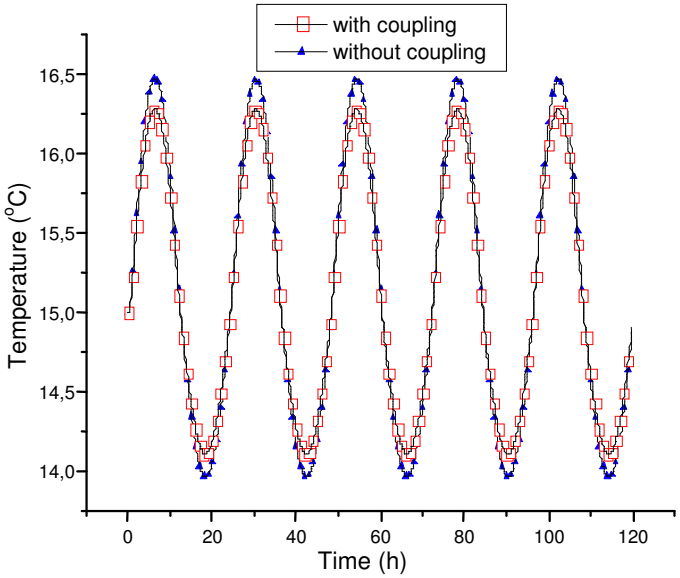

Fig. 10. Internal Temperature (Plywood).

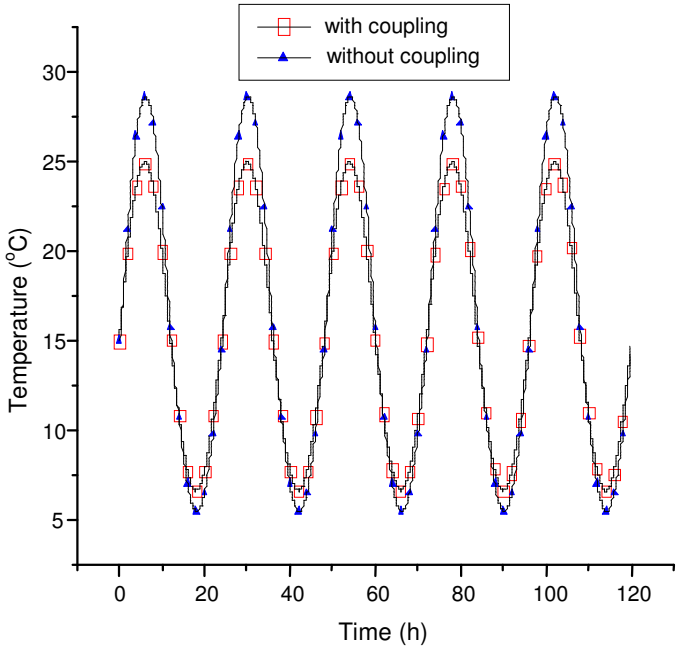

Fig. 11. External Temperature (Plywood).

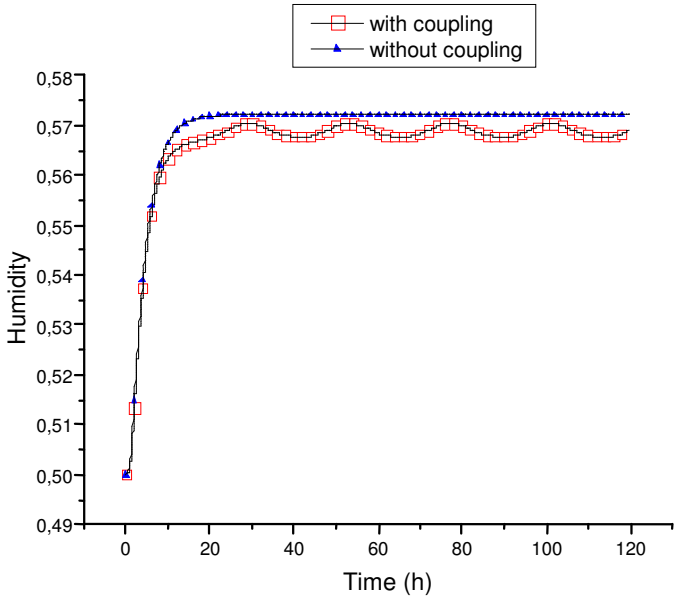

Fig. 12. Internal Humidity (Plywood).

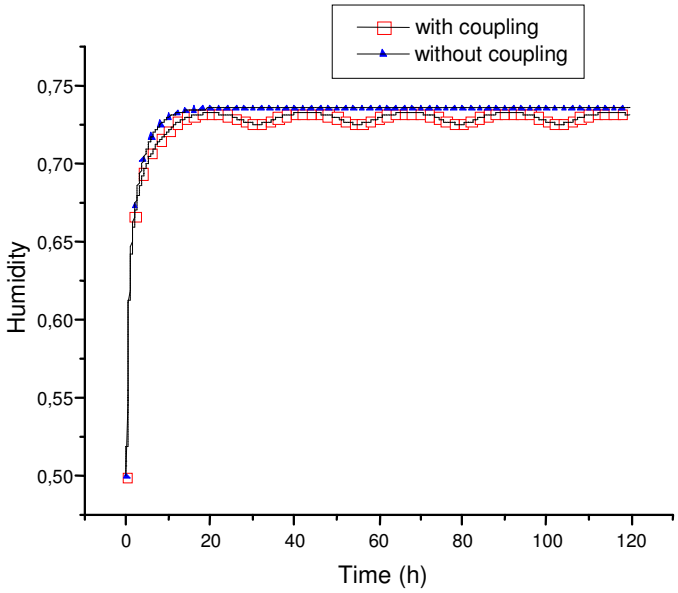

Fig. 13. External Humidity (Plywood).

Figure 14 shows that the inside temperature (x=0) is very sensitive to the variations of the thickness of the wall; its decreases with the increase of the thickness. The outside temperature (x=L) presented in Fig. 15, is less influenced by these variations of the thickness. The comparison between the two analyzed

materials shows that the thermal behaviour of the wall is identical for 10 cm thickness of the brick and 2 cm of the plywood.

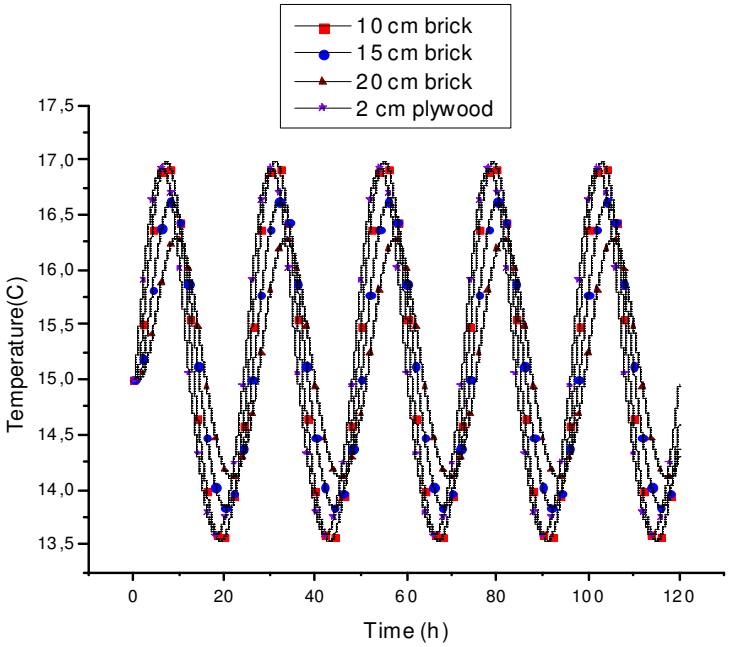

Fig. 14. Internal Temperature for Different Thicknesses of the Wall.

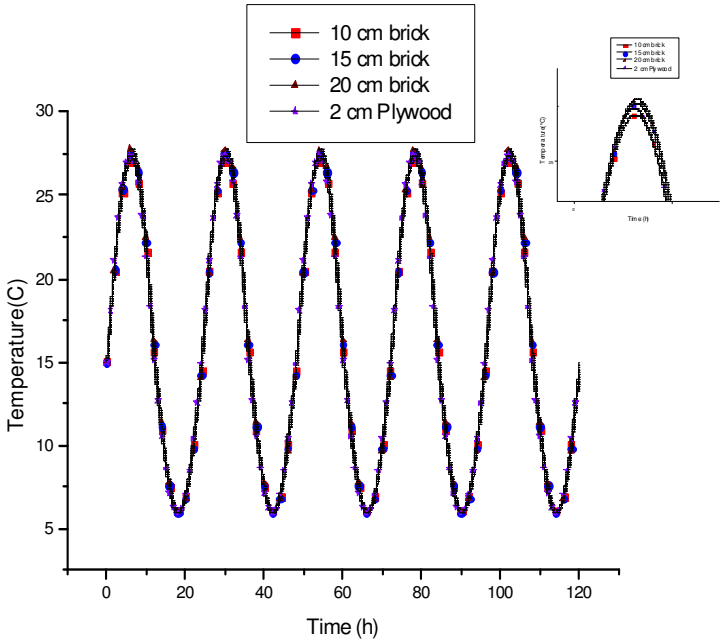

Fig. 15. External Temperature for Different Thicknesses of the Wall.

For some instants of the transient regime, we present in Figs. 16 and 17, the distribution of the temperature inside the wall.

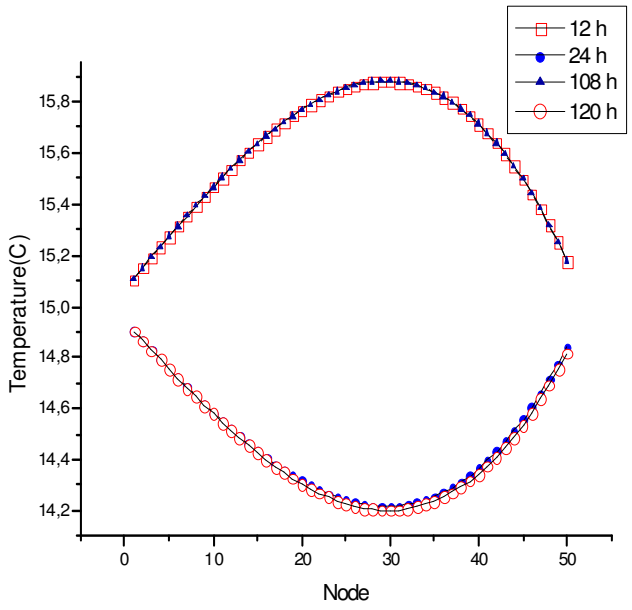

Fig. 16. Temperature Distribution at Different Times for Brick Material.

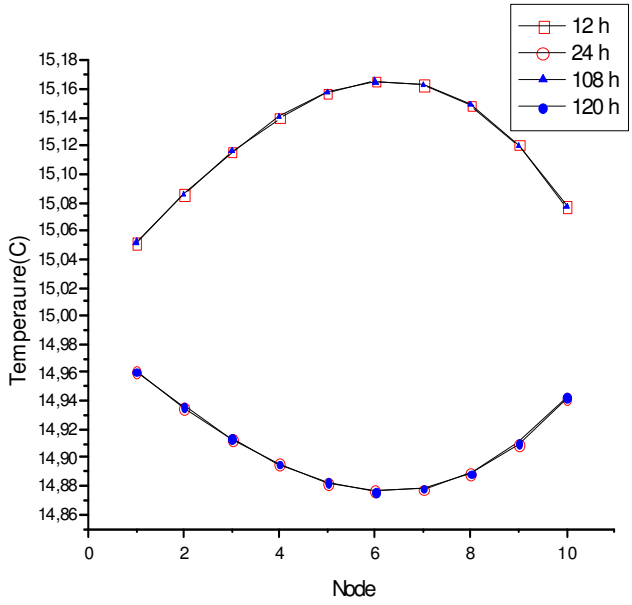

Fig. 16. Temperature Distribution at Different Times for Plywood Material.

These curves show the thermal response of the whole plate during periodic regime, particularly, we can observe that for the weak heat flux, the temperature is maximum in the middle of the wall, it is the cases of t=12 h and t=108 h and conversely, the temperature is minimum in the centre of the wall for the well brought up heat flux, see t=24 h and t=120 h. These results are agreed with those obtained in [2].

5. Conclusions

In this work, we proposed a numerical study of the transient heat and mass transfer in rectangular plate. The plate is submitted to a variable solar flux and convective heat transfer on its surface. The code developed is faster and permeated us to study the influence of different parameter. The evolutions of the distribution of the temperature and the humidity are presented for two cases of usual building materials, brick and plywood.

A comparison between coupling and no coupling heat and mass transfer approaches is presented, allowed us to see the influence of the humidity on the temperature and vice versa, in presence of variable solar flux.

The numerical results obtained show that it is possible to select and optimize the materials that make up the wall according to the objectives set in terms of temperature taking into account the interaction heat moisture and consequently in terms of electric energy consumption.

References

1. Mendes, N.; Winkelmann, F.C.; Lamberts, R.; and Philippi, P.C. (2003). Moisture effects on conduction loads. *Energy and buildings*, 35(7), 631-644
2. Mendes N.; Philipi, P.C.; and Lamberts, R. (2002). A new mathematical method to solve highly coupled equation of heat and mass transfer in porous media. *International Journal of Heat and Mass Transfer*, 45(3), 509-518.
3. Al-Sanea, S.A.; Zedan, M.F., and Al-Ajlan, S.A. (2005). Effect of electricity tariff on the optimum insulation thickness in building walls as determined by dynamic heat transfer model. *Applied Energy*, 82(4), 313-330.
4. Talukdar, P., T.; Olutmayin, S.O.; Osanyintola, O.F.; and Simonson, C.J. (2007). An experimental data set for benchmarking 1D, transient heat and moisture transfer models of hygroscopic building materials. *International Journal of Heat and Mass transfer*, 50(23-24), 4527-4539.
5. Hussain, A.; Seidel, M.A.; and Tsostas, E. (2006), Heat and mass transfer in tubular ceramic membranes for membrane reactors. *International Journal of Heat and Mass Transfer*, 49(13-14), 2239-2253.
6. Askri, F.; Jemni, B.A.; and Nasrallah, S.B. (2003). Study of two-dimensional and dynamic heat and mass transfer in a metal–hydrogen reactor. *International Journal of Hydrogen Energy*, 28(5), 537-557.
7. Oxarongo, L. (2004). *Heat and mass transfer in multiscale porous structures: Application to the study of particulate diesel filter*. Doctorate thesis, Toulouse University, Toulouse, France.
8. Hamdami, N.; Monteau, J.Y.; and Le Bail, A. (2004). Simulation of coupled heat and mass transfer during freezing of a porous humid matrix. *International Journal of Refrigeration*, 27(6), 595-603.
9. Qin, M.; Belarbi, R.; Aıt-Mokhtar, A.; and Seigneurin, A. (2006). An analytical method to calculate the coupled heat and moisture transfer in building materials. *International Communications in Heat and Mass Transfer*, 33(1), 39-48.

10. Nguyen, T.Q.; Petkovic, J.; Dangla, P.; and Baroghel-Bouny, V. (2008). Modelling of coupled ion and moisture transport in porous building materials. *Construction and Building Materials*, 22(11), 2185-2195.
11. Henriuqe dos Santos, G.; and Mendes, N. (2009). Heat, air and moisture transfer through hollow porous blocks. *International Journal of Heat and Mass Transfer*, 52(9-10), 2390-2398.
12. Zhang, Y., Lin, K.; Jiang Y.; and Zhou, G. (2008) Thermal storage and nonlinear heat transfer characteristics of PCM wallboard. *Energy and Buildings*, 40(9), 1771-1779.
13. Ordenes, M.; Lamberts, R.; and Guths, S. (2009). Estimation of thermophysical properties using signal analysis with heat and mass transfer model. *Energy and Buildings*, 41(12), 1360-1367.
14. Tamene, Y.; Abboudi, S.; and Bougriou, C. (2009). Simulation des transferts thermiques transitoires à travers un mur multicouche soumis à des conditions de flux solaire et de convection. *Revue des Energies Renouvelables*, 12(1),117-124.
15. Olalekan, F.O. (2005). *Transient moisture characteristics of spruce plywood.* Thesis. University of Saskatchewan Canada.
16. Philip, J.R.; and de Vries, D.A. (1957), Moisture movement in porous media under temperature gradients, *Transactions of American Geophysical Union*, 38, 222-232.
17. Guide to meteorological instruments and methods of observation (2008). Annexe 4-B, Formulae for the computation of measures of humidity. *World Meteorological Organization.*
18. Gerald, C.F. (1978). *Applied numerical analysis*. (7th Ed.) Addison Wesley Publishing Company.